Technical Annals

Vol 1, No 8 (2024)

Technical Annals

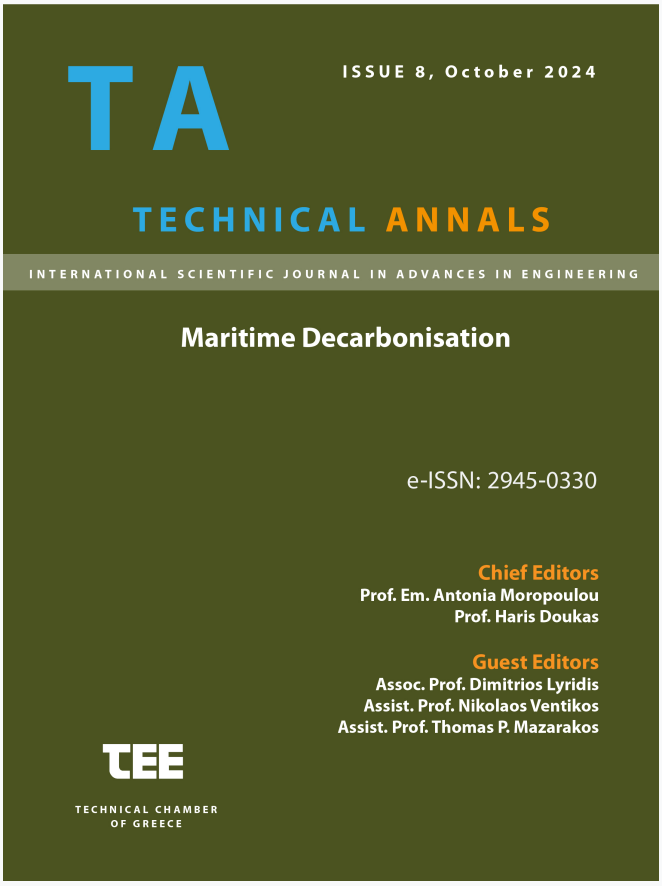

Parametric design for hydrodynamic optimization purposes: The case of "Symiaki skafi"

Sarantos Sarantidis, Thomas P. Mazarakos

doi: 10.12681/ta.40636

To cite this article:

Sarantidis, S., & Mazarakos, T. P. (2024). Parametric design for hydrodynamic optimization purposes: The case of "Symiaki skafi". *Technical Annals*, *1*(8). https://doi.org/10.12681/ta.40636

Parametric design for hydrodynamic optimization purposes: The case of "Symiaki skafi"

Sarantos P. Sarantidis[1][0009-0005-5446-7073] and Thomas P. Mazarakos[1][0000-0001-5317-2656]

[1]Department of Naval Architecture, School of Engineering, University of West Attica, Campus 1, Ag. Spyridonos 28, 12241 Egaleo, Attica, Greece
ssarantidis@uniwa.gr, tmazar@uniwa.gr

Abstract. The objective of this study is to provide a comprehensive analysis of the parametric design and hull optimization of a traditional Greek vessel known as the "Symiaki skafi". This vessel is distinguished by its unique characteristics, especially its hull geometry, which will be examined and analyzed in detail. The methodology of the manuscript is innovative. Initially, the relevant parameters affecting the design of the vessel's lines plan are delineated. Then, the positions of the control points for the parametric curves are determined. The subsequent development of the parametric surface of the model is founded on these parametric curves. The manuscript culminates in a comparative assessment of the basic hydrostatic values of the parametric model with those of the original vessel, prior to the hull optimization. This work is of dual significance in the context of decarbonization in shipping. On the one hand, it is a study of a traditional wooden vessel, which by definition has a low carbon footprint. On the other hand, it optimizes its hydrodynamic behavior so as to make it seaworthy and operationally efficient.

Keywords: Parametric analysis, traditional ship, decarbonization

1 Introduction

Hydrodynamic optimization of ship hulls plays a critical role in the decarbonization of the shipping industry. This process involves improving the hydrodynamic performance of ships, which directly affects their resistance and propulsion efficiency, reducing fuel consumption and, consequently, improving their energy efficiency [1]. This is achieved through improved hydrodynamic interactions between the hull and the propeller. Modern hydrodynamic optimization often uses computational fluid dynamics (CFD) and other simulation tools [2]. These methods enable the expeditious testing of various hull designs under varied conditions, thereby facilitating the identification of the most efficient configurations [3].

The foundations of ship parametric design and optimization trace back to the 19th century when William Froude [4], in 1861, presented a paper to the Institution of Naval Architects. He outlined similarity laws for model testing, significantly influencing ship design methodology. This led to the establishment of the first model basin in Torquay

in 1879, which became instrumental in hull form evaluation and optimization for nearly 0a century.

Murphy [5] and Mandel [6] pioneered the investigation of parametric design in shipbuilding, focusing on techniques to determine optimal solutions. A significant milestone was reached in 1982 when Lyon [7] developed a preliminary study procedure using a TI-59 calculator. Due to the computational limitations of that era, this approach avoided energy-intensive computing programs but still demonstrated the potential of structured parametric methods.

Papanikolaou [8] made further advancements in 1989 by applying parametric design to the optimization of Ro-Ro passenger ship design. By then, computational power had advanced enough to support the geometric representation of ship hulls and incorporate hydrostatic and stability calculations into design evaluations.

The latter favored the evolution in optimization techniques. Genetic algorithms were introduced by Holland [9] as an evolutionary optimization approach. However, their computational inefficiency on single-processor computers limited their early adoption. Germany saw significant contributions in the field of ship optimization through the work of Nowacki [10], and Söding [11]. Around the mid-1970s, Söding developed CHWARISMI, an optimization shell enabling ship designers to create custom optimization models. Gudenschwager [12] later expanded on this by developing DELPHI, a more user-friendly optimization shell.

Concept Exploration Models (CEMs) also emerged as an alternative to purely automated optimization. Unlike classical optimization approaches, CEMs allowed designers to visualize and analyze how different variables influenced ship performance. These models were further studied by Bertram [13] and Erikstad [14]. Several research projects involving academic institutions and industry [15], [16], facilitated the transition of optimization methodologies from research to practical industry applications. By the 2000s, commercial projects in ship hull optimization became widespread. Several researchers contributed to optimization techniques applicable to various ship types, from slow-moving tankers to high-speed semi-displacement yachts [17], [18], [19].

In this study, the "Symiaki skafi" [20], a traditional Greek vessel, was selected for analysis due to its alignment with two requirements of the International Maritime Organization (IMO) within the framework of the set of proposals for the carbon emission reduction strategy [1]. The vessel features a timber hull and wind propulsion via sails, embodying a low-impact maritime transport solution that aligns with contemporary principles of sustainable naval architecture and significantly reduces greenhouse gas emissions associated with conventional shipping.

2 Theoretical Background

Non Uniform Rational Basis Spline (NURBS) curves and surfaces constitute a numerical parametric scheme commonly used in computing engineering for the representation of 3d engineering models [21]. They are consisting of a number of appropriate control points which are in the same design area with NURBS and are mathematically interdependent with numerical equations derived from the theory of parametric curves.

A typical NURBS curve is described with the following equation:

$$\mathbf{b}(u) = \frac{\sum_{i=0}^{n}(\mathbf{b_i}w_i)N_{i,k}(u)}{\sum_{i=0}^{n} w_i N_{i,k}(u)}, \quad u_{k-1} \leq u \leq u_{n+1} \tag{1}$$

where:
$\mathbf{b}_i = (x_i, y_i, z_i)^T, i = 0,1,2, \dots \dots, n$: control points of the curve.
$w_i, i = 0,1,2, \dots, n$: the so-called control points "weights".
$N_{i,k}(u)$: B-Spline basis functions of order k defined as follow:

$$N_{i,k} = \frac{u - u_i}{u_{i+k+1} - u_i} N_{i,k-1}(u) + \frac{u_{i+k} - u}{u_{i+k} - u_{i+1}} N_{i+1,k-1}(u)$$
$$N_{i,1} = \begin{cases} 1 & u_i \leq u < u_{i+1} \\ 0 & in\ other\ case \end{cases} \tag{2}$$

$(u_0, u_1, u_2, \dots, u_m) \in [0,1]$: the elements of curve knot vector.
$m = n + d + 1$: number of elements of curve knot vectors.
d: NURBS curve degree.

From Eq. 1 it follows that a typical NURBS curve is represented in the 4d design space, using the same basis function with B-Spline parametric curves and control points of the following shape:

$$(w_i \cdot x_i, w_i \cdot y_i, w_i \cdot z_i, w_i)^T, i = 0,1, \dots \dots n$$

NURBS rational functions are given from the following equation:

$$R_{i,k}(u) = \frac{w_i N_{i,k}(u)}{\sum_{i=0}^{n} w_i N_{i,k}(u)} \tag{3}$$

Therefore, NURBS curves can also be represented by the following equation:

$$\mathbf{b}(u) = \sum_{i=0}^{n} \mathbf{b_i} R_{i,k}(u), u_{k-1} \leq u \leq u_{n+1} \tag{4}$$

n Fig. 1 a typical NURBS curve with seven control points and control points weights equal to 0.1.

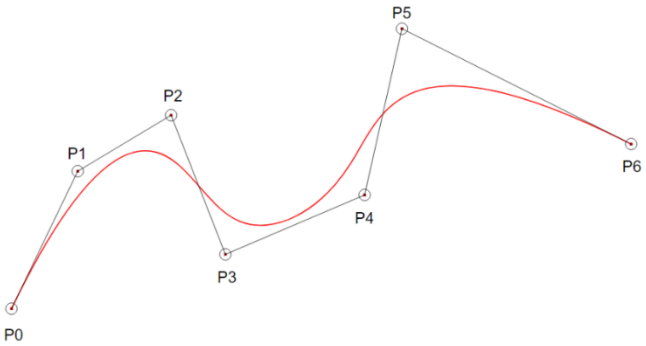

Fig. 1. Third degree NURBS curve with seven control points and $w_i = 0.1$

2.1 NURBS Curve Continuity

The geometric continuity of a NURBS curve is related to the shape smoothness and distinct in certain categories not only between the curve corresponding parts but also in the connection points with neighboring curves. The discussed continuity categories are the following:

- $\boldsymbol{G^0}$ **position continuity:** it's a zero-order continuity and observed between the individual parts of a continuous curve. In order to ensure the continuity between two neighboring curves, the start or the end point of one curve must be the same with the end or start point of the other
- $\boldsymbol{G^1}$ **tangent continuity:** it's a first-order continuity and observed when each individual curve point has a unique tangent and additional when the curve has a position continuity. In order to ensure the continuity between two neighboring curves, the connection point tangent must be the same for both the curves
- $\boldsymbol{G^2}$**curvature continuity:** it's a second-order continuity and observed when each individual curve point has a unique curvature and additional when the curve has a tangent continuity. In order to ensure the continuity between two neighboring curves, the curvature center in the connection point must be common for both the curves

The curve continuity order depends on curve degree as continuity order is smaller than it by one unit. The latter means that first-degree curves have G^0 continuity, second-degree curves have at least G^1 continuity and third-degree curves have at least G^2 continuity. This state is also affected by the knot vector unit multiplicity.

2.2 NURBS Surfaces

One NURBS surface is generally expressed as a tensor product between two NURBS curves. The general equation that presents a common NURBS surface is the following:

$$\boldsymbol{S}(u,v) = \sum_{i=0}^{n}\sum_{j=0}^{m} \mathbf{b}_{i,j} {R_{i,j}}^{k_1,k_2}(u,v) \tag{5}$$

where:

- $u_i,\ i = 0,1,2,\ldots..n+k,\ v_j\ \ j = 0,1,2,\ldots..n+k$: the knot vectors in u and v directions, respectively
- $\mathbf{b}_{i,j}$: $i = 0,1,2,\ldots,n, j = 0,1,2,\ldots,m$ the control points
- $n+1$ and $m+1$: surface control points in u and v direction respectively
- k_1 and k_2: surface orders in u and v direction respectively
- $R_{i,j}(u,v)$: surface rational functions given by the following equation:

$$\boldsymbol{R_{i,j}(u,v)} = \frac{w_{i,j}N_{i,k_1}(u)N_{j,k_2}(v)}{\sum_{i=0}^{n}\sum_{j=0}^{m} w_{i,j}N_{i,k_1}(u)N_{j,k_2}(v)} \tag{6}$$

3 Ship Parametric Design Process

In Fig. 2 the general steps of the presented parametric design procedure are presented. Each step interacts with each other and it is crucial to be mentioned that the procedure is not straight linear but has more like a circular flow and therefore a repeatability in some steps is likely to be observed.

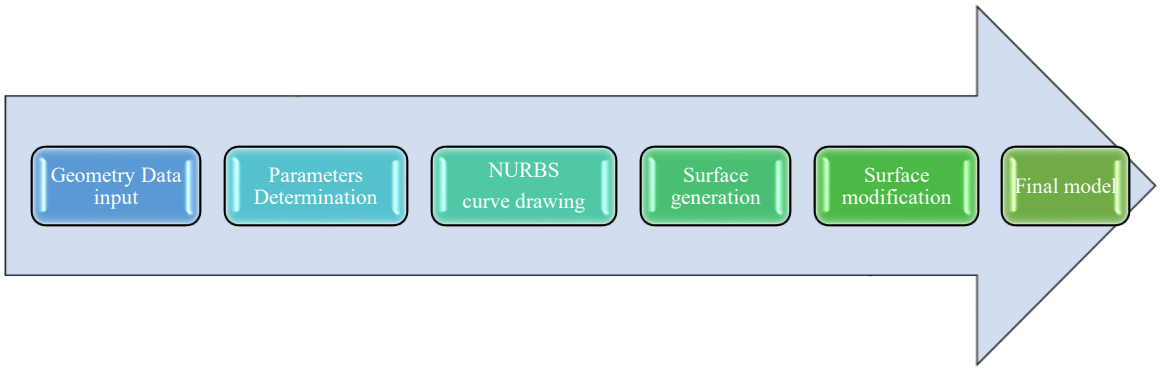

Fig. 2. Ship parametric design process

3.1 Geometry Data Input

During the ship parametric design process, geometric data (such as dimensional ratios and hull coefficients) from a sufficient number of similar existing ships must be collected to generate a preliminary base model geometry. This base model can then be modified according to the designer's requirements. Alternatively, a single existing ship—referred to as the paternal ship—can be used. In this approach, the geometry of the paternal ship is described parametrically and then modified using selected parameters, primarily for the purpose of optimizing the existing hull design.. The latter technique will be adopted in the presented method. The “Symiaki skafi” [20], a traditional Greek vessel, was selected for analysis and therefore it will be mentioned as the ship paternal. In Fig. 3 and Table 1 the selected paternal ship lines plan and main dimensions are presented.

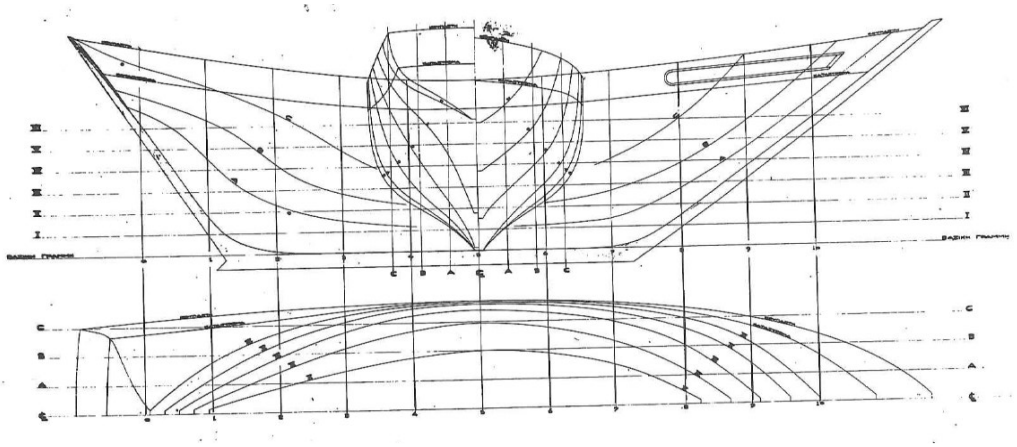

Fig. 3. Paternal ship lines plan [20]

Table 1. Paternal ship main dimensions [20]

Paternal ship main dimensions	
Length overall (m)	15
Length between perpendiculars (m)	11.7
Max breadth (m)	3.75
Depth (m)	2.5
Draught (m)	2.25

3.2 Parameters Determination

An effective ship parametric design is mainly based on the selection of the appropriate parameters, an element that requires a full understanding of the design model geometry and its operating conditions. A total of 22 parameters has been selected for the ship hull description and categorized into the following groups (see Table 2):

- **Main Parameters**: parameters that referred to the main dimensions of the designed ship hull
- **Bow Profile Parameters**: parameters that affect the designed ship bow profile geometry
- **Stern Profile Parameters**: parameters that affect the designed ship stern profile geometry
- **Midship Parameters**: parameters that affect the designed ship midship section geometry
- **Main Deck Parameters**: parameters that affect the designed ship main deck curve geometry
- **Transom Parameters**: parameters that affect the designed ship transom curve geometry

Despite the particular ship hull part, they affect, some of the selected parameters are likely to determine additional parts of the ship geometry and therefore interaction relationships between the parameters are developed (see Fig. 4-7). The latter means that a significant change of a particular parameter value might be able to imply an additional corresponding value change in different interacted parameters so the ship hull geometry not to be disturbed.

Table 2. Parameters set

Main Parameters	
LPP	Parameter that determines the ship length between perpendiculars
B/LPP	Parameter that determines the ship max breadth
D/LPP	Parameter that determines the ship depth
T/D	Parameter that determines the ship draught
Bow Profile Parameters	
LK_END/LPP	Parameter that determines the longitudinal start position of the bow profile
BOW_ANGLE	Parameter that determines the overhang angle of the bow profile with z-axis
D_BOW/D	Parameter that determines the height of the deck curve in the bow profile foremost point
Stern Profile Parameters	
LK_START/LPP	Parameter that determines the longitudinal start position of the stern profile
STERN_ANGLE	Parameter that determines the overhang angle of the stern profile with z-axis
D_STERN/D	Parameter that determines the height of the deck curve in the stern profile foremost point
Midship Parameters	
MID_LOW_PART_ANGLE	Parameter that affects the midship section low part shape
MID_UPPER_PART_ANGLE	Parameter that affects the midship section upper part shape
MID_START_TANGENT	Parameter that determines the start tangent direction of the midship section
Main Deck Parameters	
DECK_STERN_SHEER_ANGLE	Parameter that determines the main deck stern part sheer
DECK_FORE_SHEER_ANGLE	Parameter that determines the main deck fore part sheer
DECK_STERN_START_TANGENT	Parameter that determines the main deck stern part start tangent
DECK_STERN_END_TANGENT	Parameter that determines the main deck stern part end tangent
DECK_FORE_START_TANGENT	Parameter that determines the main deck fore part start tangent
DECK_FORE_END_TANGENT	Parameter that determines the main deck fore part end tangent

Transom Parameters	
TRANSOM_WIDTH/B	Parameter that determines the breadth of the transom
TRANSOM_DECK_ANGLE	Parameter that determines the transom deck angle on the xy plane
TRANSOM_CAMPER_ANGLE	Parameter that determines the transom camper angle on the yz plane

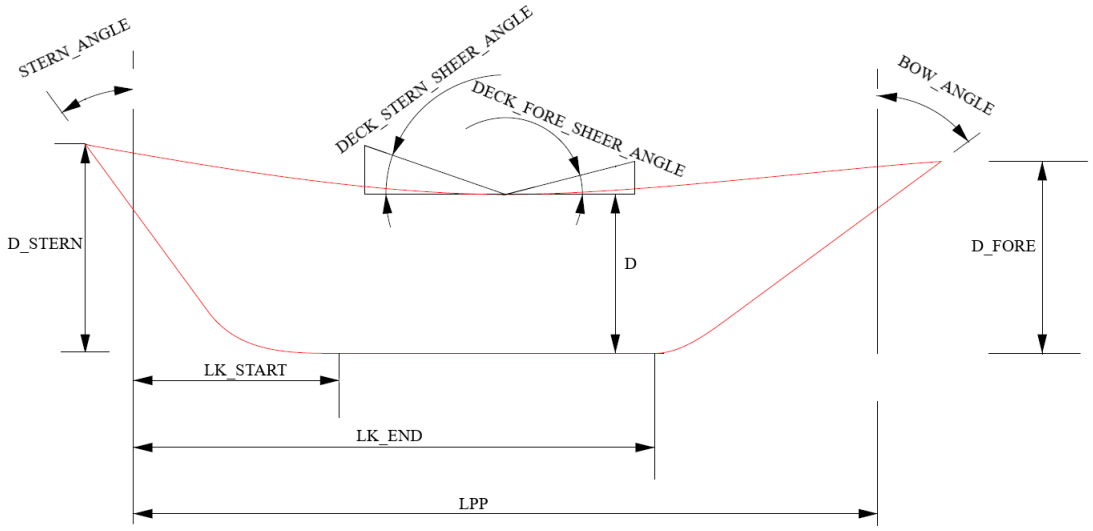

Fig. 4. Parameters that affect the profile and the side view of main deck

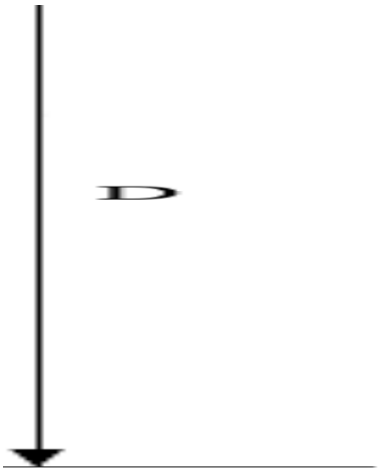

Fig. 5. Parameters that affect the midship section

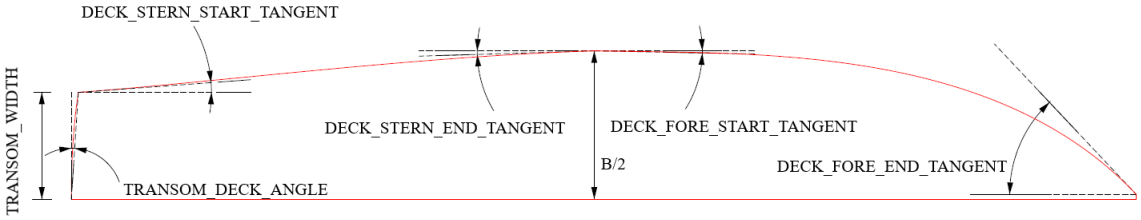

Fig. 6. Parameters that affect the top view of main deck and transom curve

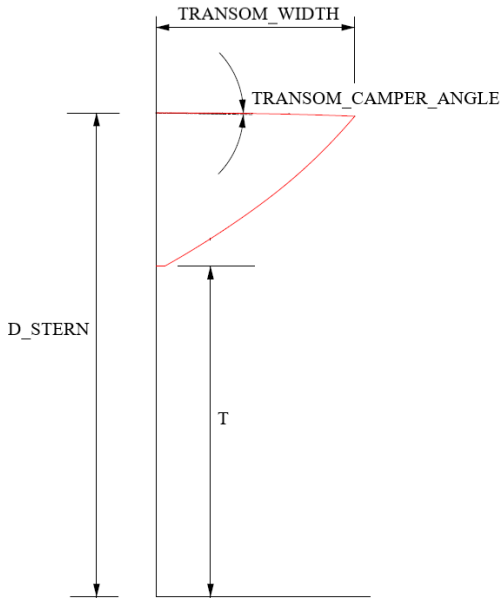

Fig. 7. Parameters that affect the front view of the transom curve

3.3 NURBS Curve Drawing

Profile curve, Midship section, Main deck curve and Transom curve consist the basic hull geometry of the designed ship model. Depending on designer requirements, changes on parameters values will significantly modify the shape of those curves and therefore leads to a completly different ship geometry.

Profile curve will be consisting of three individual curves: a curve that describes the stern profile, a curve that describes the bow profile and a line that connects the end points of the above curves and mainly represents the ship model keel length. Stern profile curve consists of two individual curves: a third-degree NURBS curve with four control points and a line (see Fig. 8). Suchlike, Bow profile curve consists of two individual curves: a third-degree NURBS curve with four control points and a line (see Fig. 9). Midship section will be represented by a fifth-degree NURBS curve with six control points (see Fig. 10). Main deck curve will be consisting of two individual curves: a third-degree NURBS curve with four control points that describes the stern part of main

deck and a third-degree NURBS curve with four control points that describes the fore part of main deck (see Fig. 11-12). Finally, Transom curve will be consisting of two individual curves: a third-degree NURBS curve with four control points that describes the camper of main deck at transom position and a third-degree NURBS curve with four interpolate points that describes the main part of Transom curve (see Fig. 13-14). In Table 3, numerical equations for the calculation of the corresponding control points coordinates are shown. An accuracy of six digits has been selected for the constant values being used in the discussed equations, in order to eliminate geometry deviations from the ship paternal and disturbances in curves continuity.

Table 3. Control points numerical equations

Stern Profile – NURBS curve part			
	x	y	z
P_0	$(LK\_START)/LPP * LPP$	0	0
P_1	$(x_{P_0} + x_{P_2})/2$	0	0
P_2	$0.686422 x_{P_0} * \tan(STERN\_ANGLE)$	0	0
P_3	$(1 - 0.200980) * x_{P_2} + 0.200980 * x_{P_4}$	0	$0.200980 * z_{P_4}$
Stern Profile – NURBS line part			
	x	y	z
P_3	x_{P_3}	0	z_{P_3}
P_4	$-0.313578 * (D/LPP * LPP) * (D\_STERN)/D * \tan(STERN\_ANGLE)$	0	$(D/LPP) * LPP * (D\_STERN/D)$
Bow Profile – NURBS curve part			
P_0	$(LK\_END)/LPP * LPP$	0	0
P_1	$L_{PP} - \tan(BOW\_ANGLE) * (D/LPP) * LPP * (D\_BOW/D)$	0	0
P_2	$(1 - 0.098039) * x_{P_1} + 0.098039 * x_{P_4}$	0	$0.098039 * z_{P_4}$
P_3	$(1 - 0.186275) * x_{P_1} + 0.186275 * x_{P_4}$	0	$0.186275 * z_{P_4}$
Bow Profile – NURBS line part			
	x	y	z
P_3	x_{P_3}	0	z_{P_3}
P_4	$L_{PP} + 0.243364 * (D/LPP * LPP) * (D\_BOW)/D * \tan(BOW\_ANGLE)$	0	$(D/LPP * LPP) * (D\_BOW)/D * \tan(BOW\_ANGLE)$
Midship section			
	x	y	z
P_0	$LPP/2$	0.06	0
P_1	$LPP/2$	$z_{P_1} * \tan(MID\_START\_TANGENT)$	$0.212 * z_{P_5}$
P_2	$LPP/2$	$0.512 * y_{P_5}$	$z_{P_3} + (y_{P_3} - y_{P_2}) * \tan(MID\_LOW\_PART\_ANGLE)$
P_3	$LPP/2$	$y_{P_5} - (z_{P_4} - z_{P_3}) * \tan(MID\_UPPER\_PART\_ANGLE)$	$0.296 * z_{P_5}$
P_4	$LPP/2$	y_{P_5}	$0.768 * z_{P_5}$
P_5	$LPP/2$	$(B/LPP) * (LPP/2)$	$(D/LPP) * LPP$

Main deck – NURBS stern part curve			
	x	y	z
P_0	$x_{P_4}(Stern\ Profile\ line\ part) + y_{P_0} * \tan(TRANSOM\_DECK\_ANGLE)$	$0.72 * (TRANSOM\_WIDTH)/B * B/LPP * LPP$	$z_{P_4}(Stern\ Profile\ line\ part) - y_{P_0} * \tan(TRANSOM\_CAMPER\_ANGLE)$
P_1	$(1 - 0.597200) * x_{P2} + 0.597200 * x_{P_4}(Stern\ Profile\ line\ part)$	$y_{P_1} + \left(x_{P_1} - x_{P_4}(Stern\ Profile\ line\ part)\right) * \tan(DECK\_STERN\_START\_TANGENT)$	$(1 - 0.597200) * z_{P2} + 0.597200 * z_{P_4}(Stern\ Profile\ line\ part)$
P_2	$x_{P_3} - \left(z_{P_0} - z_{P_3}\right) / \tan(DECK\_STERN\_SHEER\_ANGLE)$	$y_{P_3} - \left(x_{P_3} - x_{P_2}\right) * \tan(DECK\_STERN\_END\_TANGENT)$	z_{P_3}
P_3	$LPP/2$	$(B/LPP) * (LPP/2)$	$(D/LPP) * LPP$
Main deck – NURBS fore part curve			
	x	y	z
P_3	x_{P_3}	0	z_{P_3}
P_4	$x_{P_3} + \left(z_{P_4}(Bow\ Profile\ line\ part) - z_{P_3}\right) / \tan(DECK\_FORE\_SHEER\_ANGLE)$	$y_{P_3} - \left(x_{P_4} - x_{P_3}\right) * \tan(DECK\_FORE\_START\_TANGENT)$	z_{P_3}
P_5	$(1 - 0.764411) * x_{P_4} + 0.773418 * LPP$	$\left(x_{P_6} - x_{P_5}\right) * \tan(DECK\_FORE\_START\_TANGENT)$	$(1 - 0.764411) * z_{P_3} + 0.773418 * z_{P_5}$
P_6	$x_{P_4}(Stern\ Profile\ line\ part)$	0.06	$z_{P_4}(Stern\ Profile\ line\ part)$
Transom curve – Camper			
	x	y	z
P_0	$x_{P_0}(Stern\ Profile\ line\ part)$	0	$z_{P_0}(Stern\ Profile\ line\ part)$
P_1	$x_{P_0}(Stern\ Profile\ line\ part)$	$0.334158 * y_{P_3}$	$(1 - 0.022598) * z_{P_4}(Stern\ Profile\ line\ part) + 0.022598 * z_{P_3}$
P_2	$(1 - 0.231625) * x_{P_0} + 0.231625 * x_{P_3}$	$0.669388 * y_{P_3}$	$(1 - 0.211031) * z_{P_4}(Stern\ Profile\ line\ part) + 0.211031 * z_{P_3}$
P_3	$x_{P_0}(Main\ deck\ stern\ part)$	$y_{P_0}(Main\ deck\ stern\ part)$	$z_{P_0}(Main\ deck\ stern\ part)$
Transom curve – Main frame			
	x	y	z
P_3	x_{P_3}	y_{P_3}	z_{P_3}
P_4	$(1 - 0.630041) * x_{P_6} + 0.630041 * x_{P_4}(Stern\ Profile\ line\ part)$	$0.533333 * (B/LPP) * (LPP/2)$	Appropriate intersection with stern profile curve
P_5	$(1 - 0.260721) * x_{P_6} + 0.260721 * x_{P_4}(Stern\ Profile\ line\ part)$	$0.266667 * (B/LPP) * (LPP/2)$	Appropriate intersection with stern profile curve
P_6	Appropriate intersection with stern profile curve	0.06	$(T/D) * (D/LPP) * LPP$

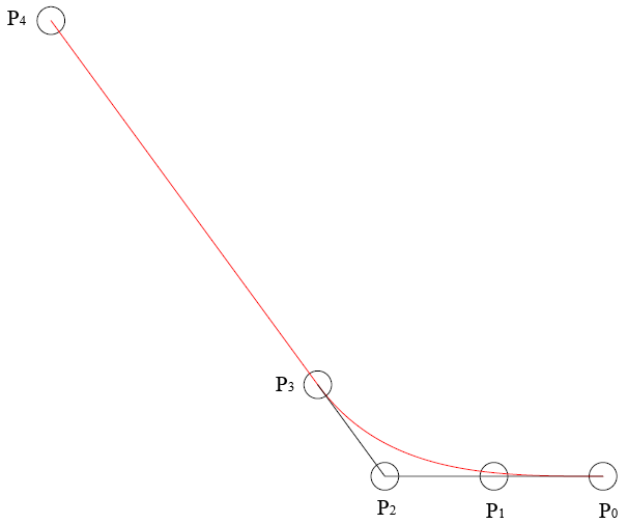

Fig. 8. Stern profile curve control points

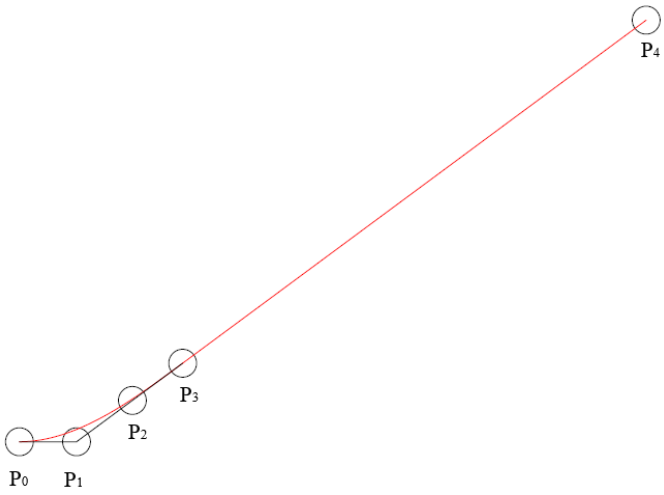

Fig. 9. Bow profile curve control points

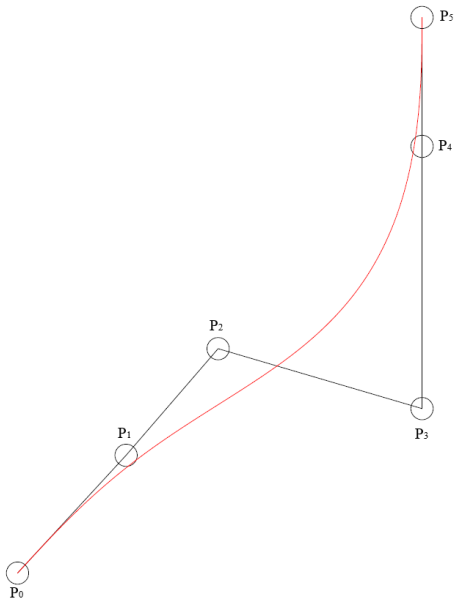

Fig. 10. Midship section control points

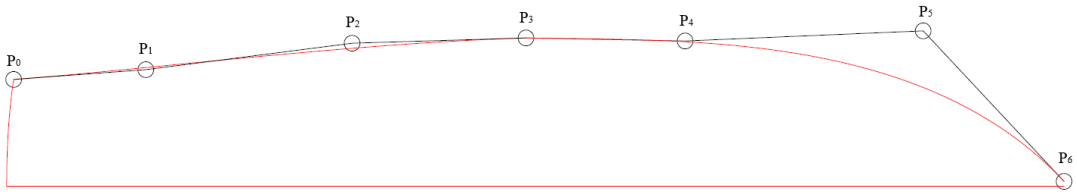

Fig. 11. Main deck curve control points (top view)

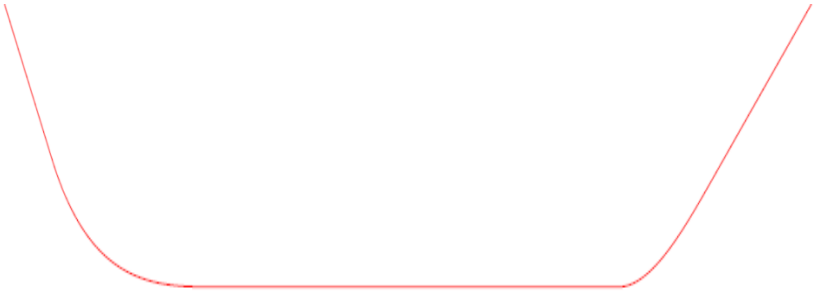

Fig. 12. Main deck curve control points (side view)

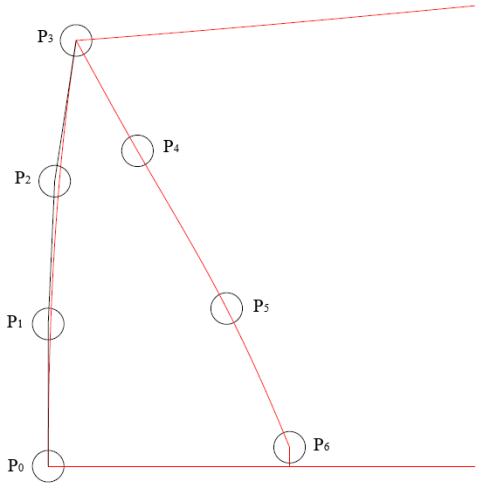

Fig. 13. Transom curve control points (top view)

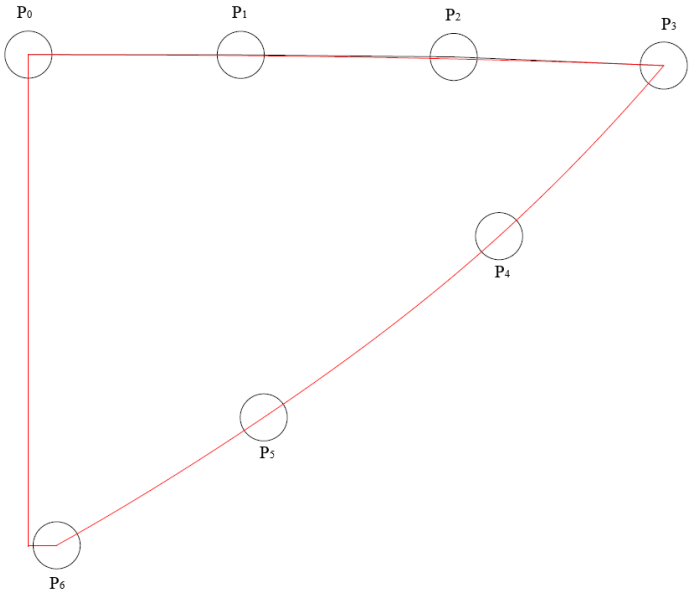

Fig. 14. Transom curve control points (front view)

After having completed the description of the basic geometry of the designed model, next step deals with the drawing of additional proper curves (frames or stations) in which the ship hull surface will be developed. The number and the shape of these curves must not only ensure the accuracy of ship geometry description but also the design simplification. Therefore, a total of 14 additional curves have been drawn in certain longitudinal positions (frames or stations). As they are presented in Fig. 15, each curve

is extracted from the paternal ship hull and be rebuild into a fifth-degree NURBS curve with six control points, which are determined by certain numerical equations that evolve the midship, profile and main deck curve corresponding control points.

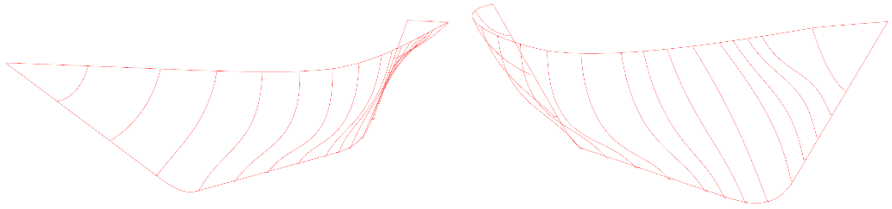

Fig. 15. Ship model frames

It should be mentioned that the designed ship frames (as well as the main deck fore part) have a flat part between their first control point (last control point in case of main deck fore part curve) and the ship profile curve. The latter is represented by a perpendicular line that connects the corresponding control point with the ship profile curve as it's shown in Fig. 17.

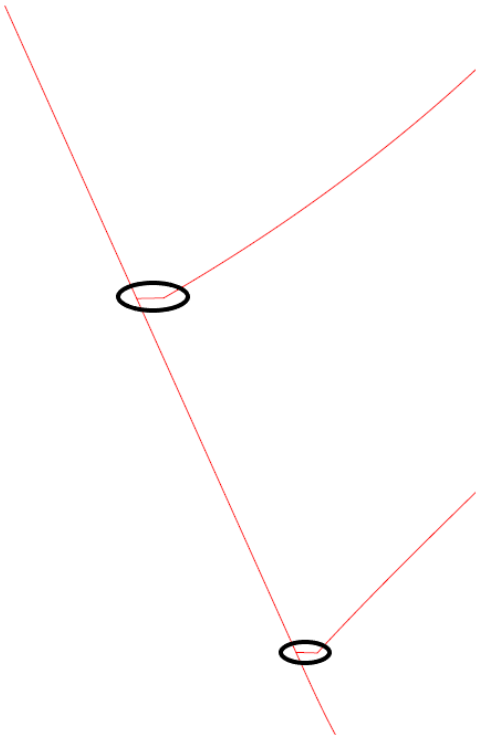

Fig. 16. Frames flat part

3.4 Surface

Based on the curve framework that been described in the previous paragraph and with the aid of the Computer Aided Designed program Rhinoceros [22] the ship hull surface is generated as it's shown in Fig. 17.

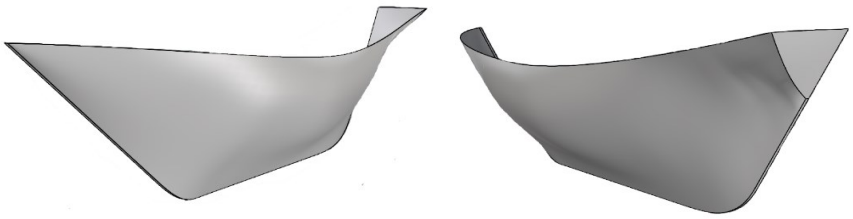

Fig. 17. Ship hull surface

One of ship parametric design requirements is that the produced hull surface to have a G^1 tangent continuity and be smooth. In the presented case, the ship hull surface consists of three parts: the main part (which is produced by the frames, the main deck curve and the connected edge with the flat part surface), the transom surface and the flat part surface. Between these three parts, a G^0 position continuity is generally accepted. In order to ensure the G^1 tangent continuity in the main surface area, the latter will be generated as one piece, with the aid of Rhinoceros Curve Network command using Profile Curve, Main Curve, Transom Curve and the 14 additional curves (frames) as guides. However, this method may burden the surface smoothness.

In order to reduce the main surface creases the following method is implied: first a mesh is created based on the surface geometry (see Fig. 18) and then with the aim of the appropriate computing program commands, creases are eliminated and the mesh is refined to a quadrilateral form based-recursive subdivision described by Catmull and Clark [23] (see Fig. 19). Then, a set of new frames are extracted by intersections with mesh surface at certain longitudinal positions (see Fig. 20). Finally, the refined surface main part is produced based on the new frames and profile, main deck and transom curve (see Fig. 21).

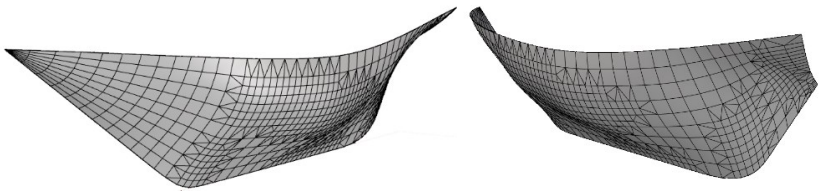

Fig. 18. Surface based mesh geometry

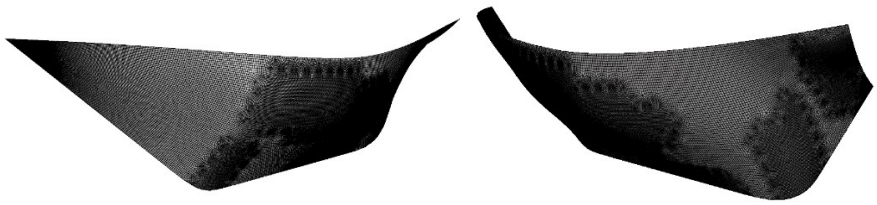

Fig. 19. Refined quadrilateral mesh

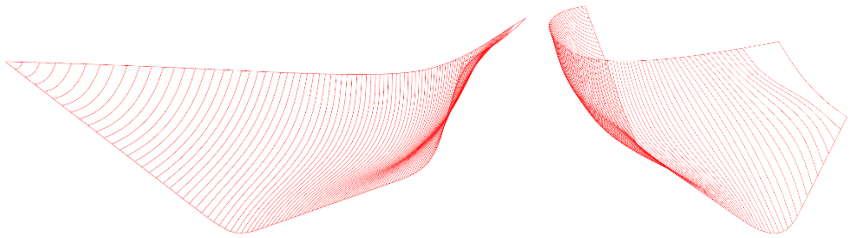

Fig. 20. New set of frames

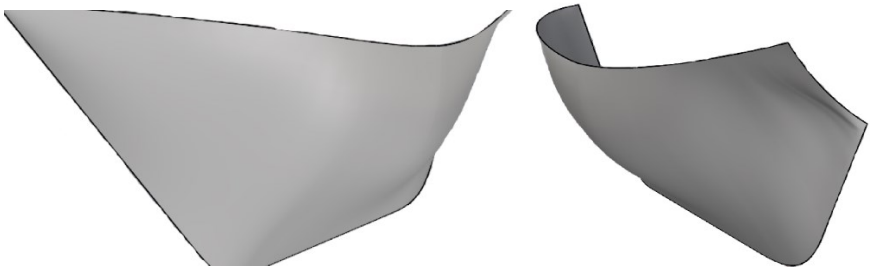

Fig. 21. Refined surface main part

4 Results

Parameters values have been modified in such way, so that the ship paternal hull surface produced in first place will serve as a criterion for parametric design accuracy. Nevertheless, different values should be possible to be given to the selected parameters for the investigation of new geometries, for possible ship hull optimization goals and

for possible limitations in the parameters value range in order to prevent possible geometry disturbances. In Fig. 22-24 the final ship hull surface is presented.

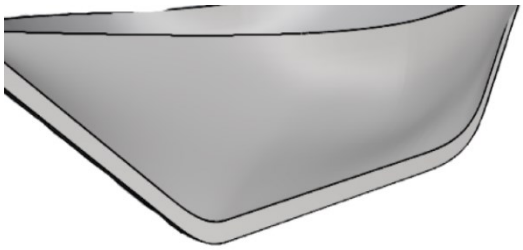

Fig. 22. Ship hull surface (perspective view)

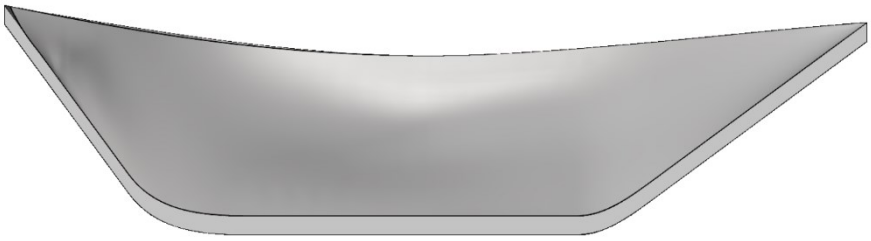

Fig. 23. Ship hull surface (side view)

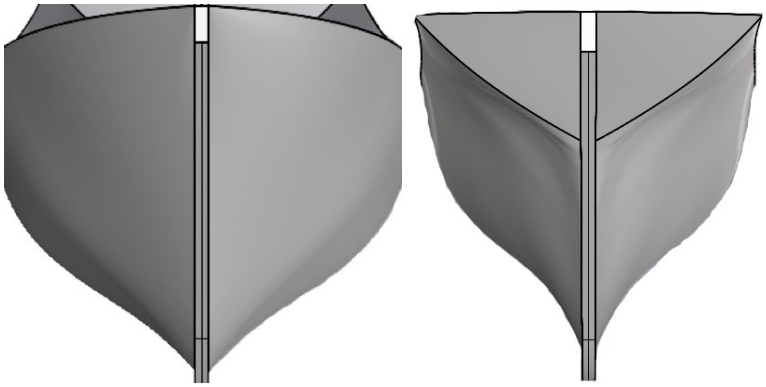

Fig. 24. Ship hull surface (front view).

In Fig. 25-26 ship parametric model lines plan are presented. A small deviation is observed between the waterlines of parametric model and the paternal ship which may possibly be due to the number of frames been extracted from the refined mesh surface. On the other hand, theoretical frames of the parametric model are similar to those of the paternal ship.

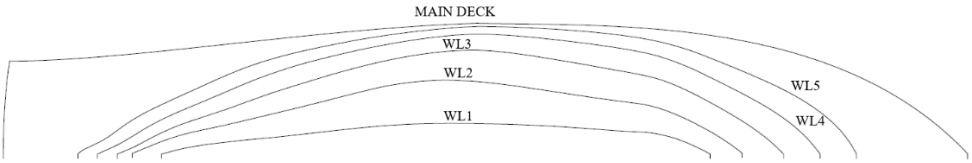

Fig. 25. Ship parametric model lines plan (waterlines)

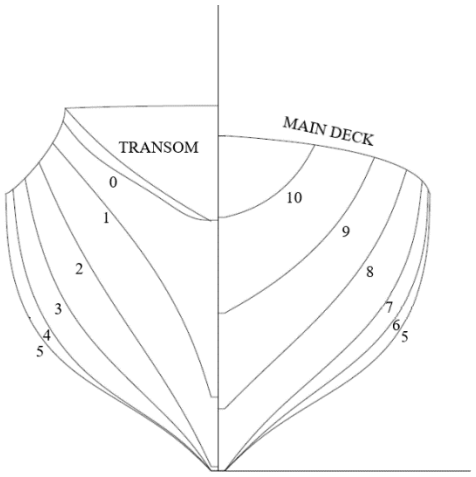

Fig. 26. Ship parametric model lines plan (frames)

In Table 4 hydrostatics comparison between parametric model and the paternal ship is presented. With the exception of LCB deviation, every other hydrostatic deviation is small and within accepted limits.

Table 4. Hydrostatics comparison

Hydrostatics			
	Parametric model	Ship paternal	Deviation (%)
$\nabla(m^3)$	39.358	39.615	0.19
LCB(m)	-0.022	-0.02	10
AWL(m^2)	32.705	32.790	0.26
LCF(m)	0.149	0.155	3.87

AM(m^2)	5.695	5.705	0.18
C_B	0.402	0.403	0.25
C_M	0.675	0.676	0.15
C_{WL}	0.749	0.751	0.27
LB(m)	1.485	1.486	0.07
BM(m)	0.707	0.712	0.70

5 Conclusions

The central focus of this research was on the parametric design for hydrodynamic optimization of a traditional ship hull, the "Symiaki skafi." The study had as a fundamental premise that the traditional character of the vessel has the primary role and therefore the interventions should not alter its characteristics to the point of deviating too much from its traditional lines. It is understood that in the case of traditional boats, the ideal balance must be found between traditional design and optimal hydrodynamic design.

Advanced computational tools and parametric analysis were employed to identify the critical parameters that affect the performance of the traditional ship. The conclusions derived from this research underscore the significance of parametric analysis in optimizing ship design.

The implementation of these methodologies holds considerable potential to benefit the shipping industry, including the reduction of operating costs and the enhancement of environmental performance. The advancement of sophisticated computational models, along with the integration of artificial intelligence, has the potential to further refine decision-making processes in the domains of ship design and construction, thereby contributing to the advancement of the shipbuilding industry as a whole.

The integration of contemporary computational tools within the domain of traditional shipbuilding has the potential to enhance the sustainability of this sector, thereby opening a new field of maritime operations for traditional ships and achieving a substantial reduction in carbon emissions in Greek maritime transport.

References

1. International Maritime Organization (IMO). 2023 IMO Strategy on Reduction of GHG Emissions from Ships: https://www.imo.org/en/OurWork/Environment/Pages/2023-IMO-Strategy-on-Reduction-of-GHG-Emissions-from-Ships.aspx. (2023)
2. Mallouppas, G., Yfantis, E.A.: Decarbonization in Shipping Industry: A Review of Research, Technology Development, and Innovation Proposals. J. Mar. Sci. Eng. 9, (415). https://doi.org/10.3390/jmse9040415 (2021)
3. Kim, H., Yang, C., Noblesse, F.: Hull form optimization for reduced resistance and improved seakeeping via practical designed-oriented CFD tools, (375-385) (2010)
4. Froude, W.: On the rolling of ships, Institution of Naval Architects (1861)

5. Murphy, R. D., Sabat, D. J., Taylor, R. J.: Least cost ship characteristics by computer techniques. Marine Technology 2(2), 174-202 (1963)
6. Mandel, P., Leopold, R.: Optimization Methods Applied to Ship Design, Trans. of SNAME 74 (1966)
7. Lyon, T.D.: A Calculator–Based Preliminary Ship Design Procedure. Marine Tech-nology 19(2), 140-158 (1982)
8. Papanikolaou, A., Nowacki, H., Zarafonitis, G., Kraus, A., Androulakis, M.: Concept design and optimization of a SWATH passenger/car ferry. In: Proceedings, IMAS 89, Marine Management (Holdings) Ltd., London (1989)
9. Holland, J.: Adaptation in natural and artificial systems, University of Michigan Press (1975)
10. Nowacki, H.: Five decades of Computer-Aided Ship Design, Computer-Aided Design 42 (11), 956-969 (2010)
11. Söding, H.: Resistance decrease by computer-aided hull shape improvements. In: 2nd Conf. High-Performance Marine Vehicles, Hamburg, 431-445 (2011)
12. Gudenschwager,H.: Application and optimization in basic ship design, OPTIMISTIC – Optimization in Marine Design, Mensch & Buch Verlag, Berlin, 173-190 (2003)
13. Bertram, V.: Optimization in ship design, OPTIMISTIC – Optimization in Marine Design, Mensch & Buch Verlag, Berlin, .29-56 (2003)
14. Erikstad, S.: A decision support model for preliminary ship design, PhD thesis, Uni-versity of Trondheim (1996)
15. Maisonneuve, J.: Towards ship performance improvement using modeFRONTIER. In: 5th Num. Towing Tank Symp. (NuTTS), Pornichet (2002)
16. Valdenazzi, F., Harries, S., Janson, C. E., Leer-Andersen, M., Maisonneuve, J. J. Marzi, J., Raven, H.: The FANTASTIC RoRo: CFD Optimisation of the forebody and its experimental verification. In: Int. Conf. Ship and Shipping Research (NAV. 2003), Palermo (2003)
17. Dudson, E., Harries, S.: Hydrodynamic fine-tuning of a pentamaran for high-speed sea transportation services. In: Int. Conf. Fast Sea Transporta-tion (FAST), St. Petersburg (2005)
18. Hutchison, B.L., Hochkirch, K.: CFD hull form optimization of a 12,000 cu.yd. (9175 m3) dredge. In: 10th Int. Symp. Practical Design of Ships and Other Floating Struc-tures (PRADS), Houston (2007)
19. Harries, S., ValdenazzI, F., ABT, C., Viviani, U.: Investigation on optimization strategies for the hydrodynamic design of fast ferries. In: 6th Int. Conf. Fast Sea Transportation (FAST), Southampton (2001)
20. Antoniou, A.: Research on the Naval Data of the Greek Type Vessels, PhD Thesis, National Technical University of Athens, Greece (1969)
21. Kostas, K.: 3d design & calculations with the aim of Rhino 3d, DaVinci Publication, Athens, Greece (2014)
22. McNeel, R.: Rhinoceros 3D, Version 8.0. Robert McNeel \& Associates, Seattle, WA (2010)
23. Clark, J., Catmull, E.: Recursively generated b-spline surfaces on arbitrary topological meshes, Computer-Aided Design 10(6), 350-355 (1978)